From Chaos to Quasi-Periodicity

Alexander P. Kuznetsov[1,2], Natalia A. Migunova[2], Igor R. Sataev[1], Yuliya V. Sedova[1] and Ludmila V. Turukina[1,2]

[1] *Kotel'nikov's Institute of Radio-Engineering and Electronics of RAS, Saratov Branch, Zelenaya str., 38, Saratov, 410019, Russian Federation*

[2] *Saratov State University, Astrakhanskaya str., 83, Saratov, 410012, Russian Federation*

E-mail: apkuz@rambler.ru, migunovanatasha@mail.ru, sataevir@rambler.ru, sedovayv@yandex.ru, lvtur@rambler.ru

Abstract

Ensembles of several Rössler chaotic oscillators are considered. We show that a typical phenomenon for such systems is an emergence of different and sufficiently high dimensional invariant tori. The possibility of a quasi-periodic Hopf bifurcation and a cascade of such bifurcations based on tori of increasing dimension is demonstrated. The domains of resonance tori are revealed. Boundaries of these domains correspond to the saddle-node bifurcations. Inside the domains of resonance modes, torus-doubling bifurcations and destruction of tori are observed.

Keywords: Chaos; Quasi-periodic oscillation; Invariant torus; Lyapunov exponent; Bifurcation
Mathematical Subject Classifications: 70K43, 65P20, 65P30, 34D08

1 Introduction

The problem of interaction between oscillators is a topic of interest in various fields of physics, chemistry and biology [1-8]. The simplest case is when the individual oscillators exhibit periodic oscillations. Their interaction can lead to either synchronization or quasi-periodic oscillations. With an increase in the number of oscillators in the system, a number of possible incommensurate frequencies increases. As a result, multi-frequency quasi-periodic oscillations may arise. The invariant tori of higher dimension correspond to these oscillations [9-15]. With an increase in the coupling, the tori can be destroyed with the formation of chaos. In this paper, we discuss an alternative situation. We consider a system of a small number of coupled chaotic oscillators and demonstrate an occurrence of the invariant tori of different dimensions with an increase in the coupling.

The possibility of the quasi-periodic oscillations in coupled systems with chaos was discussed in [16-18]. An effect of the coupling on the amplitude dynamics of two coupled Rössler chaotic oscillators was considered in [16], where the possibility of a two-frequency quasi-periodicity was also discussed. However, a detailed investigation was not done. In [17-18], the ring of three identical unidirectionally coupled Lorenz systems was investigated. Not only two-, but also three-frequency quasi-periodic regimes were revealed. But only the one-parameter analysis was performed. Three-frequency tori were detected in a very narrow range of the parameter (about one thousandth). The emergence of a new frequency was explained in [17,18] by the possibility of rotational motion of the system and its high degree of symmetry associated with the identity of the interacting subsystems.

In this paper, the chains and the networks of a small number of the Rössler chaotic oscillators are considered. It is essential that the oscillators are non-identical by the frequency parameter. It is known that for two such oscillators both synchronous and asynchronous chaotic regimes are possible [19-21]. An approximate location of the domains of these regimes in the frequency mismatch – coupling parameter plane was considered in [19,21]. In fact, a detailed analysis of this parameter plane reveals its sufficiently complex structure. With an increase in the number of oscillators, the synchronization picture becomes much more complicated. An appropriate analysis is the subject of this paper. For the completeness of investigation, we start from the case of two coupled oscillators, and then consider a chain of three coupled oscillators. After that, we investigate a network of four and five os-

cillators. A variety of possible dynamical regimes in the system grows with an increase in the number of oscillators. Two-parameter Lyapunov analysis is usable for the proper investigation [12-15,22-23]. It allows to identify quasi-periodic regimes of different dimensions and hyperchaos with different number of the Lyapunov exponents. Another problem discussed in this paper is a possible type of bifurcations of invariant tori. We find the quasi-periodic Hopf bifurcations, which correspond to a soft appearance of the torus of higher dimension [24]. The saddle-node bifurcations are also possible. They are typical when the resonance tori arise on the surface of a torus of higher dimension.

2 Two coupled chaotic oscillators

Consider a system of two coupled Rössler oscillators [19-21]:

$$\begin{array}{ll} \dot{x}_1 = -(1-\Delta)y_1 - z_1, & \dot{x}_2 = -(1+\Delta)y_2 - z_2, \\ \dot{y}_1 = (1-\Delta)x_1 + py_1 + \mu(y_2 - y_1), & \dot{y}_2 = (1+\Delta)x_2 + py_2 + \mu(y_1 - y_2), \\ \dot{z}_1 = q + (x_1 - r)z_1, & \dot{z}_2 = q + (x_2 - r)z_2. \end{array} \tag{1}$$

Here *x, y, z* are the dynamic variables, Δ is the frequency mismatch. The parameters are set to be $p = 0.15$, $q = 0.4$, $r = 8.5$. This corresponds to the chaotic regime in the individual subsystems.

Let us determine a localization of different dynamical regimes in the frequency mismatch – coupling parameter plane (Δ, μ). To do this, we calculate the spectrum of Lyapunov exponents of the system (1) at each point in the parameter plane, and then we color this plane according to the spectrum structure [12-15,23]. As a result, the following regimes are visualized: P – periodic regime (one zero exponent), T2 – two-frequency quasi-periodic regime (two zero exponents), C – chaos (one positive exponent) and HC – hyperchaos (two positive exponents).

Fig. 1 shows a chart of Lyapunov exponents in the (Δ, μ) parameter plane[1]. Inside the domain of periodic regimes P, there is a complete synchronization of oscillators. For large values of Δ, there are oscillations with a limit cycle which has one fixed point in the Poincaré section (period 1). With an increase in Δ, this cycle undergoes a period-doubling bifurcations (period 2,

[1]Compare Fig. 1 with Fig. 2 in [20].

4, etc.), and then a synchronous chaos occurs. To the right of these domains, an amplitude death domain (AD) is located where self-oscillations are suppressed by the dissipative coupling. In this case, all Lyapunov exponents are negative.

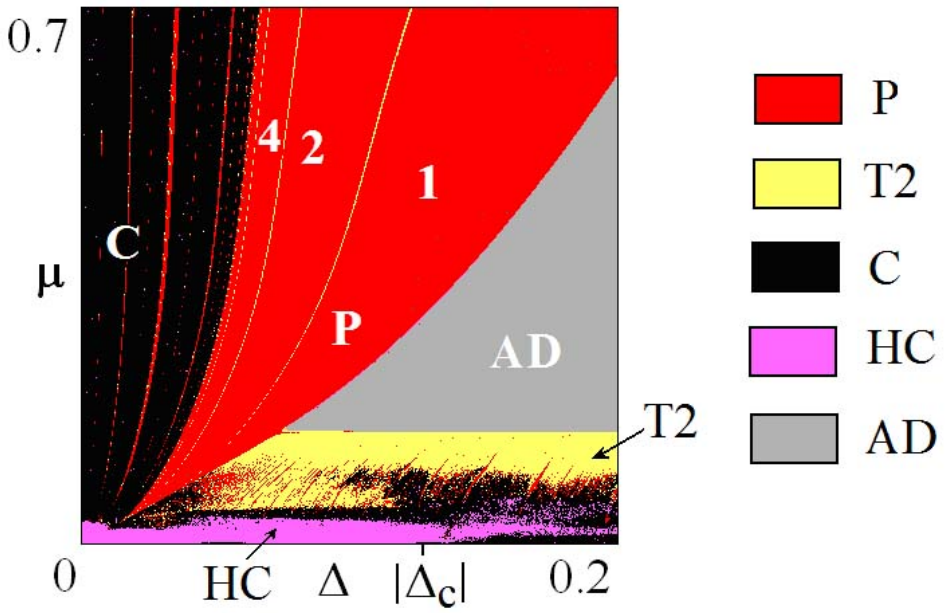

Figure 1: Chart of Lyapunov exponents for the system (1). The color palette is discussed in the text and presented to the right of the figure. Numbers indicate periods of the system in regime of periodic oscillations (i.e. periods evaluated as the number of steps in the Poincaré section required for the repeating of the system's state).

Below the AD domain, asynchronous regimes arise. At small coupling, there is hyperchaos, because the system without coupling is divided into two chaotic oscillators, each having a positive Lyapunov exponent. With an increase in the coupling, hyperchaos is changed to an ordinary chaos. Further increase in coupling leads to the appearance of two-frequency quasi-periodicity. Thus, the coupling suppresses the chaotic component, but retains the classical beatings that are typical for the interacting self-oscillating systems with limit cycles.

Portraits of attractors plotted in the Poincaré section[2] for the increased coupling values are presented in Fig. 2. We can see a transition from hyperchaos HC to chaos C with further appearance of an invariant curve corresponding to the two-frequency quasi-periodicity T2.

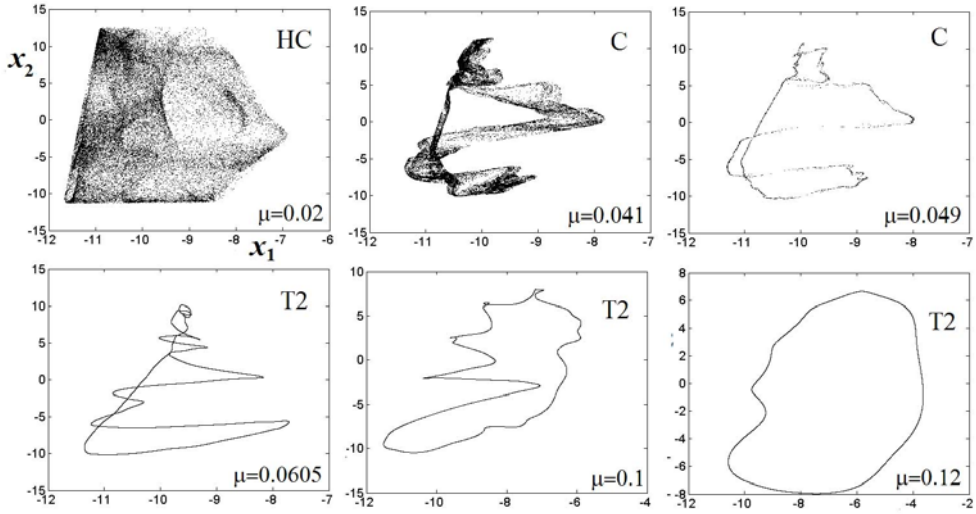

Figure 2: Evolution of an attractor of the system (1) in the Poincaré section with an increase in the coupling, Δ=0.085.

Thus, there is a "self-oscillating component" in the dynamics of chaotic oscillators which becomes apparent and initiates quasi-periodic oscillations when the dissipative coupling is introduced. It can be expected that this component will also become apparent with an increase in the number of oscillators. To show this, we consider a chain of three coupled chaotic oscillators. But at first, one more thing should be discussed.

When the coupling is absent, the equations of individual subsystems are not the strict Rössler equations due to the factor Δ. This factor is responsible for the oscillation frequency. At the same time, variation of Δ results in the changing of an excitation degree [20]. This fact is illustrated in Fig. 3 where the bifurcation tree for an individual oscillator is shown. One can see that the chaos disappears at $\Delta_C < -0.13$. For the coupled oscillators (1), it results in the appearance of an ordinary chaos instead of hyperchaos at $\Delta >$

[2]Hereinafter Poincaré section corresponds to the intersection between phase trajectories and the surface $y_1 = 0$, $x_1 < 0$.

$|\Delta_C|$ in Fig. 1, because oscillations in the second subsystem become regular. However, the domain of two-frequency quasi-periodicity is maintained and weakly depends on this effect. Note that the presence of periodic windows in a bifurcation diagram is a typical phenomenon for the chaotic oscillators and becomes apparent in the dynamics of ensembles of coupled non-identical oscillators. When we discuss network of several elements, we will return to this property.

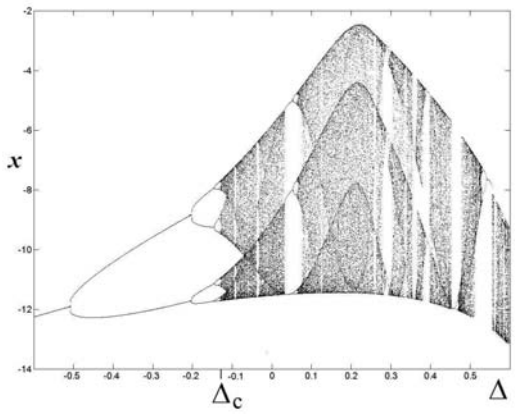

Figure 3: Bifurcation diagram of the individual oscillator for $r = 8.5$.

3 Three Rössler chaotic oscillators

Now consider a chain of three coupled Rössler oscillators:

$$
\begin{aligned}
&\dot{x}_1 = -y_1 - z_1,\\
&\dot{y}_1 = x_1 + py_1 + \mu(y_2 - y_1),\\
&\dot{z}_1 = q + (x_1 - r)z_1,\\
&\\
&\dot{x}_2 = -(1-\Delta_1)y_2 - z_2,\\
&\dot{y}_2 = (1-\Delta_1)x_2 + py_2 + \mu(y_1 + y_3 - 2y_2),\\
&\dot{z}_2 = q + (x_2 - r)z_2,\\
&\\
&\dot{x}_3 = -(1-\Delta_2)y_3 - z_3,\\
&\dot{y}_3 = (1-\Delta_2)x_3 + py_3 + \mu(y_2 - y_3),\\
&\dot{z}_3 = q + (x_3 - r)z_3.
\end{aligned}
\qquad (2)
$$

Here Δ_1 is the frequency mismatch between the first and second oscillators, Δ_2 is the frequency mismatch between the first and third oscillators.

A plot of the four largest Lyapunov exponents as a function of the coupling parameter μ for the system (2) is shown in Fig. 4 for $\Delta_1 = 0.56$, $\Delta_2 = 0.05$. One can see that not only two-frequency T2, but also three-frequency T3 regimes with three zero Lyapunov exponents are possible.

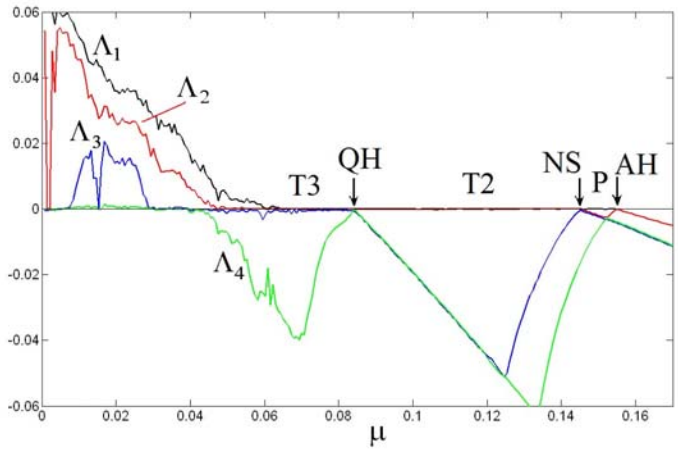

Figure 4: Plot of the largest Lyapunov exponents as a function of the coupling parameter for three coupled chaotic oscillators (2). AH denotes the Andronov–Hopf bifurcation, NS is the Neimark–Sacker bifurcation, QH corresponds to the quasi-periodic Hopf bifurcation. Values of the parameters are $\Delta_1 = 0.56$, $\Delta_2 = 0.05$.

With a decrease in μ, there is a following sequence of bifurcations in Fig. 4. At first, a stable limit cycle arises as a result of the Andronov–Hopf bifurcation AH, and one zero Lyapunov exponent $\Lambda_1 = 0$ appears. Then, a soft birth of a two-frequency torus occurs which is caused by the Neimark–Sacker bifurcation NS and characterized by two zero exponents $\Lambda_1 = \Lambda_2 = 0$. The further decrease in μ leads to a birth of a three-frequency torus with three zero Lyapunov exponents[3]. This is caused by the quasi-periodic Hopf bifurcation QH [25] and easily detected in Fig. 4: before the bifurcation point, the third and fourth exponents coincide, $\Lambda_3 = \Lambda_4$. At the point QH, the third Lyapunov exponent becomes zero, $\Lambda_3 = 0$, and the fourth one

[3]The precision in numerical evaluations of zero exponents is up to 10^{-7}.

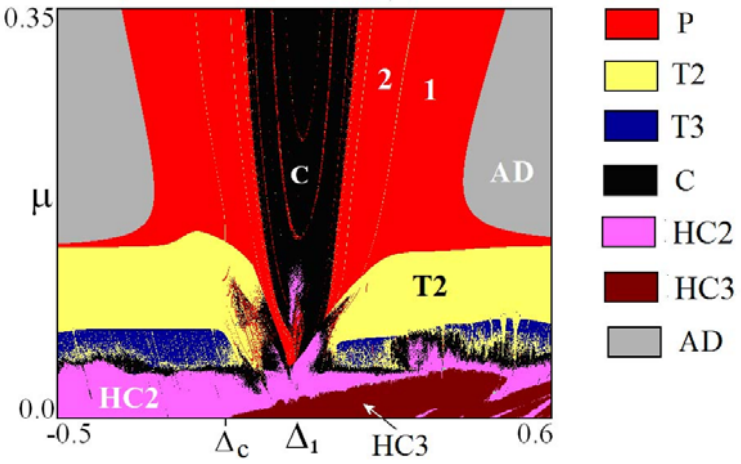

Figure 5: Chart of Lyapunov exponents for three coupled Rössler chaotic oscillators (1). TN denotes the quasi-periodic regime with N incommensurable frequencies. HCN corresponds to the hyperchaos with N positive Lyapunov exponents. Values of the parameters are $p = 0.15$, $q = 0.4$, $r = 2.5$, $\Delta_2 = 0.05$.

becomes negative again. This is a characteristic feature of this bifurcation responsible for a soft birth of a three-frequency torus [25].

Two-parameter Lyapunov analysis reveals a distribution of regimes shown in Fig. 5. The domains of two- and three-frequency quasi-periodic regimes are sufficiently wide as well as the chaotic and hyperchaotic ones.

The examples of portraits of attractors plotted in the Poincaré section for the increased coupling values μ are given in Fig. 6. Discuss them and start with the case of large μ. Fig. 6i represents a two-frequency torus T2 with an invariant curve close to a circle in the Poincaré section. With a decrease in μ, a soft birth of a three-frequency torus T3 from the invariant curve occurs, as is shown in Fig. 6h. The further decrease in μ results in occurrence of the invariant curves corresponding to the two-frequency resonance tori. An example is shown in Fig. 6g. If we decrease slightly the coupling value (only by 0.0001), a three-frequency torus occurs abruptly. Interleaving of trajectories giving rise to this torus is clearly visible on its surface in Fig. 6f. This occurs as a result of the hard saddle-node bifurcation of invariant tori.

With further decrease in μ, one can see in Fig. 6d an invariant curve having complex shape. This curve corresponds to one of the possible two-

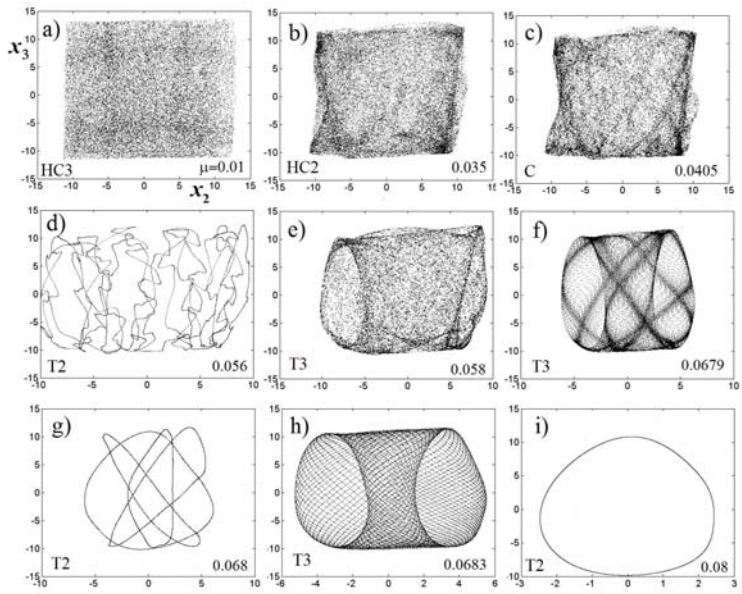

Figure 6: Portraits of attractors plotted in the Poincaré section for three coupled Rössler chaotic oscillators (2); $\Delta_1 = 0.19$, $\Delta_2 = 0.05$.

frequency resonance tori. Note that the number of resonance windows is sufficiently large[4]. Finally, for small coupling, the tori are destroyed with an emergence of chaos and then hyperchaos, Fig. 6a-c.

Fig. 7 represents the Fourier spectra of quasi-periodic oscillations for three coupled chaotic oscillators. The parameter values are the same as in Fig. 6h and Fig. 6i. Fig. 7a shows the spectrum of three-frequency quasi-periodic oscillations obtained at a lower value of μ. Fig. 7b refers to the two-frequency oscillations at higher coupling value. One can see the characteristic spectrum arrangements which are typical for the quasi-periodic oscillations with the proper number of incommensurate frequencies.

With an increase in the frequency parameter Δ_1, the common picture remains the same, but the difference between the oscillation frequencies becomes stronger. This fact is evident in the Poincaré section of the three-frequency torus given in Fig. 8.

[4]It is significantly larger than that for three coupled oscillators (2) in case of regular oscillations in the subsystems. This results in a visual perception that the three-frequency domain contains almost no two-frequency synchronization tongues.

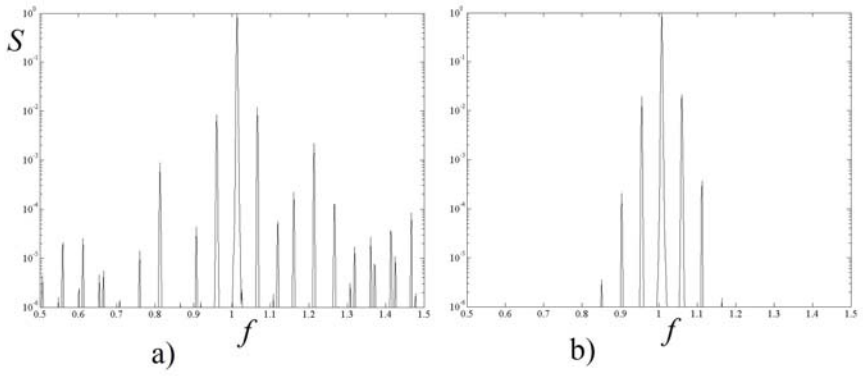

Figure 7: Oscillation spectra for three coupled Rössler chaotic oscillators (2) plotted inside the quasi-periodic domain; a) $\mu = 0.0683$, b) $\mu = 0.08$.

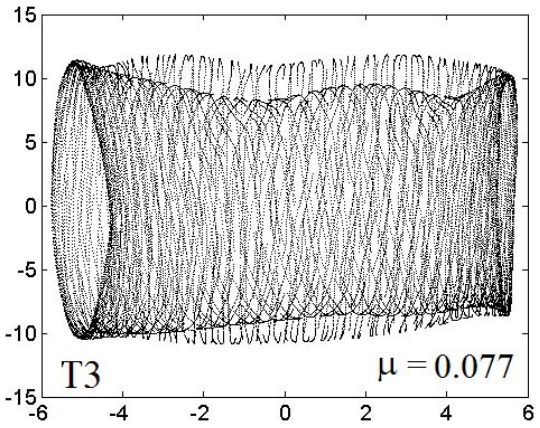

Figure 8: Poincaré section of the three-frequency torus for the system (2); $\Delta_1 = 0.56$, $\Delta_2 = 0.05$.

Fig. 9 shows the bifurcation diagram, i.e. the set of all values of the variable x_1 for different values of the coupling parameter on the attractor in the chosen Poincaré section. This diagram illustrates bifurcations responsible for the occurrence of invariant tori of different dimensions. At the point NS, the Neimark–Sacker bifurcation NS occurs and a two-frequency torus is born. At this point, a single "branch", which corresponds to the limit cycle, becomes so wide that a set of points at given μ occupies a finite interval of x_1-values. At lower values of μ, the windows of resonance limit cycles are

clearly visible. At the point QH, the bifurcation diagram becomes abruptly wider again. This is the quasi-periodic Hopf bifurcation point [25], at which a soft birth of a three-frequency torus from a two-frequency torus occurs.

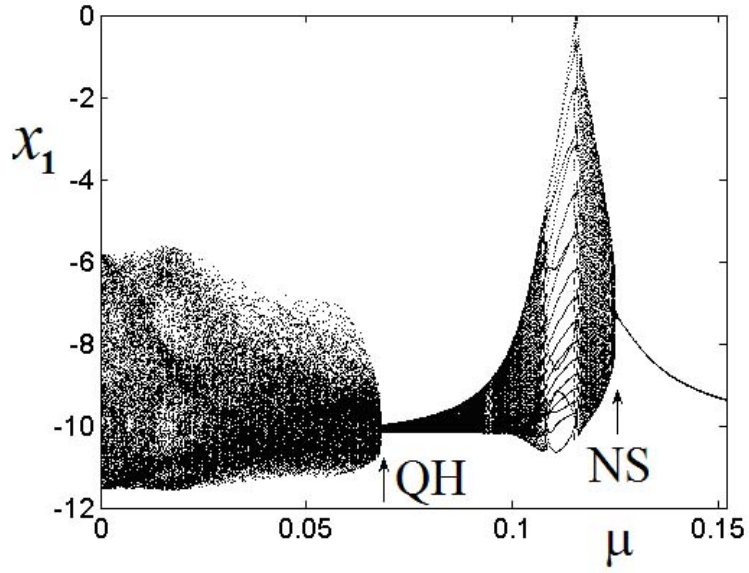

Figure 9: Bifurcation diagram for three coupled Rössler chaotic oscillators (2); $\Delta_1 = 0.19$, $\Delta_2 = 0.05$.

Now discuss the transition region from chaos to three- and two-frequency tori in the parameter plane. An enlarged fragment of the chart of Lyapunov exponents is given in Fig. 10. This figure illustrates an embedded system of resonance tongues of two-frequency tori in the domain of three-frequency regimes. The tips of these tongues are immersed now in the chaotic domain and are destroyed.

Examples of portraits of attractors plotted in the Poincaré section inside the resonance tongue are given in Fig. 11. Above the quasi-periodic Hopf bifurcation QH, an invariant curve is close to a circle, Fig. 11a. Then, it becomes more complicated, Fig. 11b. With a decrease in the coupling μ, one can see a doubling bifurcation of an invariant curve inside the resonance tongue, Fig. 11c. Note that this bifurcation line is partially visible on the chart as a set of blue points inside the tongue, because one of the Lyapunov exponents becomes zero at the bifurcation moment. The further decrease in

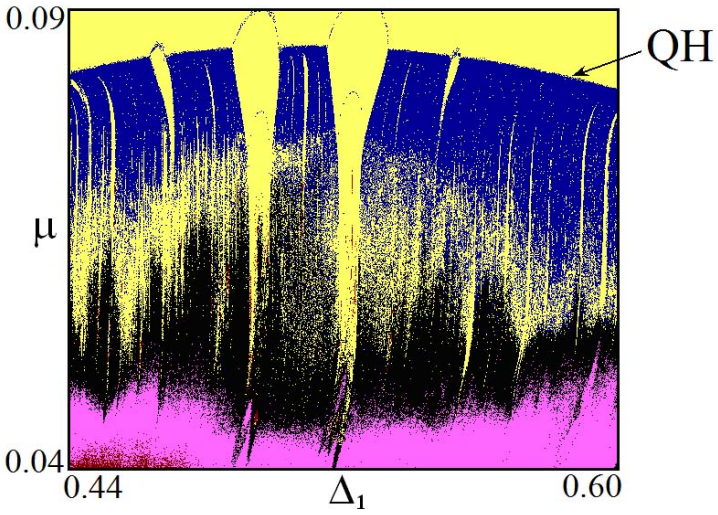

Figure 10: Enlarged fragment of the chart of Lyapunov exponents shown in Fig. 5.

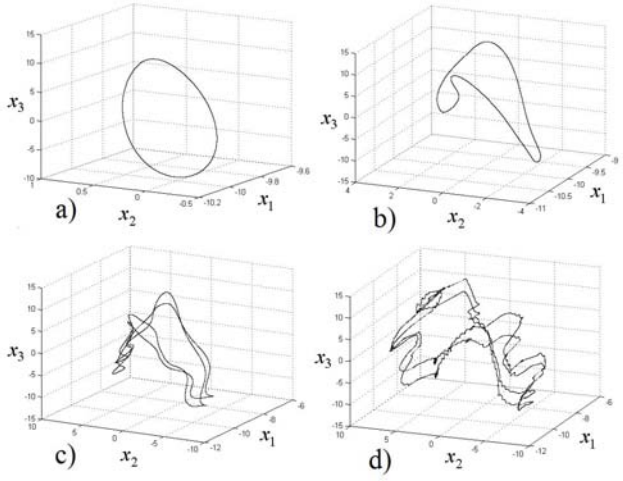

Figure 11: Portraits of attractors plotted in the Poincaré section for the system (1) inside the domain of two-frequency resonance torus; a) $\Delta_1 = 0.514$, $\mu = 0.089$, b) $\Delta_1 = 0.522$, $\mu = 0.084$, c) $\Delta_1 = 0.522$, $\mu = 0.076$, d) $\Delta_1 = 0.52$, $\mu = 0.06$.

μ results in the destruction of a two-frequency invariant torus illustrated in Fig. 11d.

4 Network of four Rössler chaotic oscillators

Now we consider a more complex system, a network of four chaotic oscillators:

$$\begin{aligned} \dot{x}_n &= -(1+\tfrac{n-1}{3}\Delta)y_n - z_n, \\ \dot{y}_n &= (1+\tfrac{n-1}{3}\Delta)x_n + py_n + \tfrac{\mu}{3}\textstyle\sum_{i=1}^{4}(y_i - y_n), \\ \dot{z}_n &= q + (x_n - r_n)z_n. \end{aligned} \tag{3}$$

In this case, the individual oscillators have equidistant frequencies, and an increase in Δ results in an increase in the frequency mismatch between all oscillators.

The chart of Lyapunov exponents for the system (3) is shown in Fig. 12. Different colors indicate periodic regimes P, quasi-periodic regimes T with a different number of incommensurate frequencies, chaos C and hyperchaos CH with a different number of positive exponents. The color palette is given in the figure to the right.

First, we discuss the domain of asynchronous regimes at sufficiently large frequency mismatches. At the low coupling, hyperchaos with four positive Lyapunov exponents HC4 is dominant. It is quite natural for a system of four chaotic oscillators. With an increase in the couling, the number of positive exponents decreases gradually, and an ordinary chaos C occurs after the HC3 and HC2 transition. At higher μ, a complex alternating pattern of different regimes is observed. Here, two-frequency tori T2 and three-frequency tori T3 are typical.

This fact is illustrated in Fig. 13 by plotting the largest Lyapunov exponents as a function of the coupling parameter for $\Delta = 0.25$. One can see a possibility of a two-frequency torus T2 at the large coupling. With a decrease in μ, a three-frequency torus occurs as a result of the quasi-periodic Hopf bifurcation. Windows of two-frequency resonance tori are also clearly visible on the plot. They are marked by arrows. Their boundaries correspond to saddle-node bifurcations of tori.

Four-frequency tori are also possible, but they are less typical. They are reliably identified at high frequency mismatches. The corresponding plot of five largest Lyapunov exponents is shown in Fig. 14 for $\Delta = 0.5$. At large coupling, there is a stable steady state. Then, it turns into a stable limit

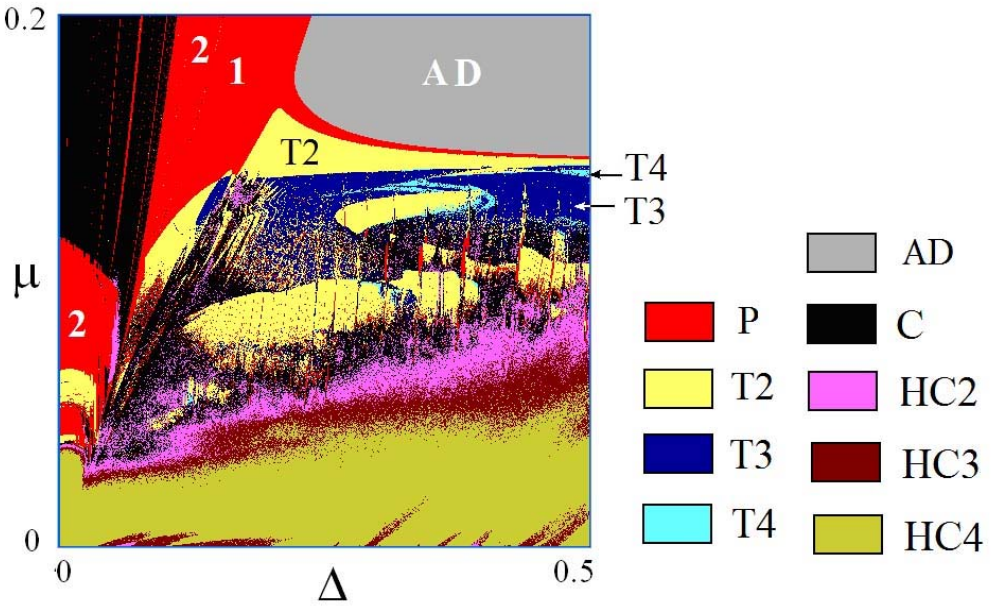

Figure 12: Chart of Lyapunov exponents for the network of four chaotic oscillators (3); $p = 0.15$, $q = 0.4$, $r = 8.5$.

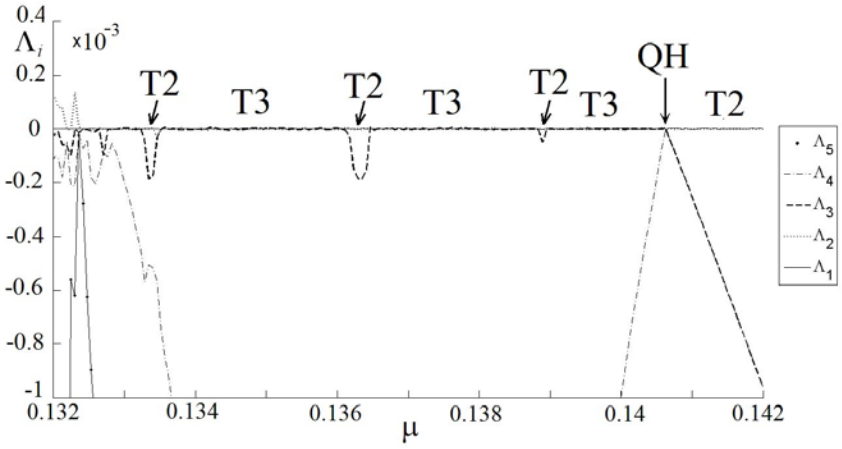

Figure 13: Plot of five largest Lyapunov exponents as a function of the coupling parameter and characteristic bifurcation points for the system of four coupled Rössler chaotic oscillators (3) at $\Delta = 0.25$.

cycle via the Andronov–Hopf bifurcation AH. This limit cycle turns into a two-frequency torus at the Neimark–Sacker bifurcation point NS. A three-frequency torus arises at the quasi-periodic bifurcation point QH1. The third and fourth Lyapunov exponents coincide ($\Lambda_3 = \Lambda_4$) before the bifurcation point and equal to zero at this point. Then, the third exponent remains zero, and the fourth one becomes negative again, which is typical for this type of bifurcation [25]. As a result of a similar bifurcation QH2, a four-frequency torus occurs at lower μ. Before this bifurcation, the fourth and fifth exponents coincide, $\Lambda_4 = \Lambda_5$.

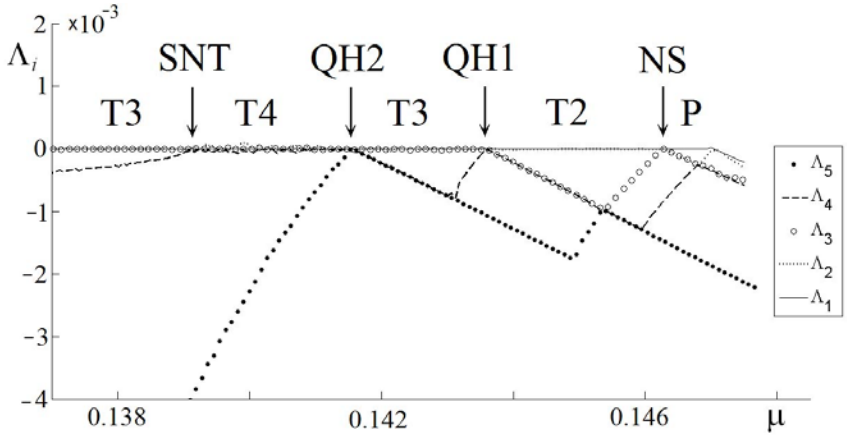

Figure 14: Plot of five largest Lyapunov exponents as a function of the coupling parameter and characteristic bifurcation points for the system of four coupled Rössler chaotic oscillators (3) at $\Delta = 0.5$.

Fig. 15 shows the Fourier spectrum and portrait in the Poincaré section for the four-frequency torus. We can see that the spectrum consists of the individual lines, and the four fundamental components are visible. Other components correspond to the combination frequencies.

Let us return to Fig. 14. With further decrease in the coupling, the saddle-node bifurcation of tori SNT occurs. This bifurcation results in a reduction of the torus dimension, and a three-frequency resonant torus arises. In this case, the fifth Lyapunov exponent always remains negative, which defines another type of bifurcation [25].

Thus, at high frequency mismatches the observed bifurcation scenario begins as the Landau–Hopf scenario with a decrease in the coupling [14,26-

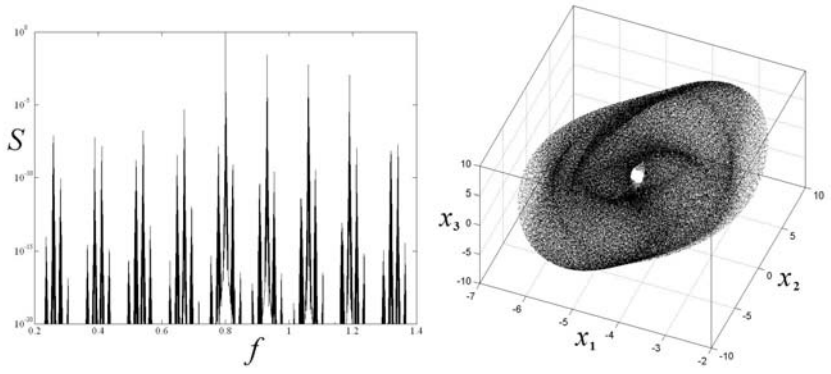

Figure 15: Fourier spectrum and portrait in the Poincaré section for the system of four coupled Rössler chaotic oscillators (3) inside the domain of four-frequency torus at $\Delta = 0.5$, $\mu = 0.14$.

27]. Then, however, a three-frequency resonant torus occurs. An appearance of chaos at lower values of the coupling is caused by the destruction of this torus.

In the intermediate frequency mismatch range (between $\Delta \approx 0.25 - 0.5$) on the chart of Lyapunov exponents in Fig. 12, the domains of four-frequency tori are also visible. It can be clearly seen in the plot of Lyapunov exponents in Fig. 16. In this case, there is a kind of interaction between the resonances of different types. For example, a three-frequency resonance torus arises on the surface of a four-frequency torus with an increase in the coupling, see Fig. 16. Then, however, a two-frequency resonance torus occurs on its surface. Thus, a whole hierarchy of different resonances is possible.

Fig. 16 reveals also the specific regimes, which correspond to the two-frequency tori with a very small Lyapunov exponent. This exponent decreases slowly with a decrease in the coupling. For example, see the left domain of two-frequency tori T2 in Fig. 16.

5 Synchronous and asynchronous quasi-periodicity

We have discussed only asynchronous regimes which occur in the system (3) at sufficiently large frequency mismatch Δ. However, synchronous regimes

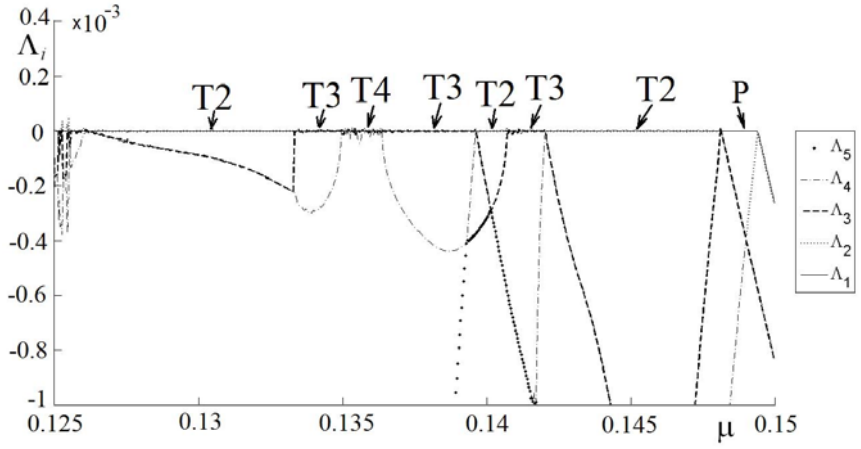

Figure 16: Plot of five largest Lyapunov exponents as a function of the coupling parameter for the system of four coupled Rössler chaotic oscillators (3) at $\Delta = 0.375$.

have also some new interesting features. For the two chaotic oscillators, a synchronous regime can be periodic or chaotic [19-21]. For the system (3) at the low frequency mismatch, both periodic and chaotic regimes are also possible, see Fig. 12. However, we can see also on the chart in Fig. 12 that a quasi-periodic regime arises on the basis of the 2-period regime. Fig. 17 illustrates this fact. The corresponding Poincaré section of the doubled two-frequency torus is shown in Fig. 17, right. At the same time, the regime is synchronous from the point of view of the phase dynamics. To verify this, consider the time dependences of the relative phases of the oscillators in Fig. 17. Here, φ_i is the phase of the i-th oscillator defined as the simple geometric phase [19-21]. We can see that all three relative phases oscillate within a limited range. Thus, all phases are captured. However, the regime is quasi-periodic. The physical nature of such synchronous quasi-periodicity consists in changing the relative phases with some extra frequency rhythm.

For comparison purpose, Fig. 18 shows a similar plot for the sufficiently large frequency mismatch Δ. In this case, the regime is also quasi-periodic, but only relative phases of the first and second, third and fourth oscillators are mutually captured. The relative phase of the second and third oscillators increases indefinitely (or changes in the whole range from 0 to 2π if consider 2π-periodicity of the phase). To distinguish this regime, we call it

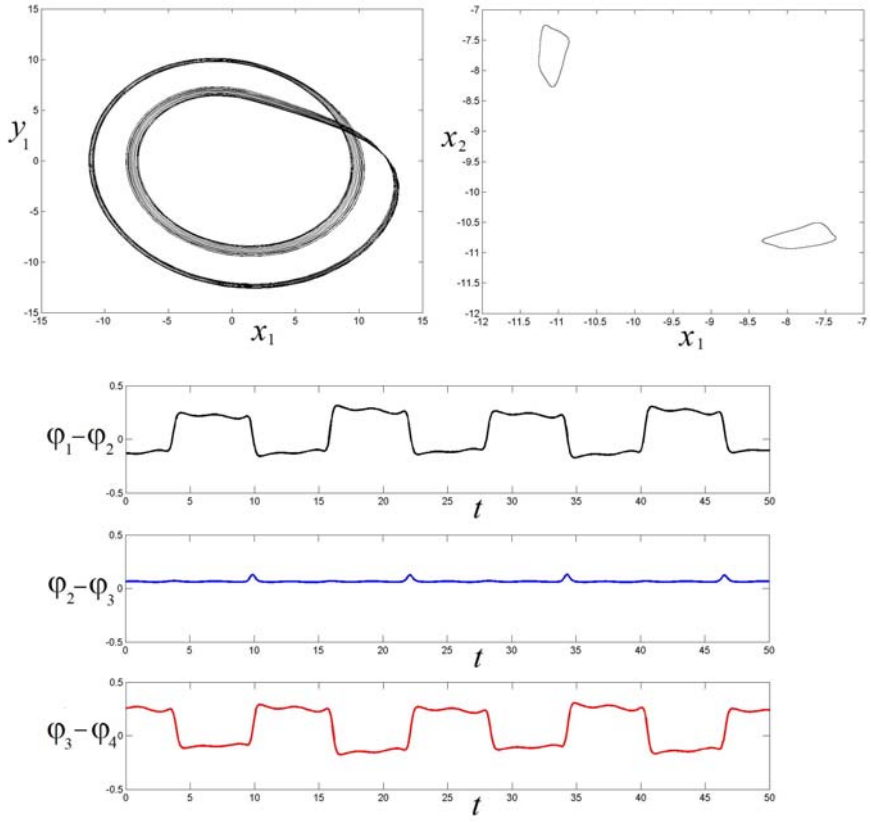

Figure 17: Phase portrait, Poincaré section and plots of three relative phases as functions of time at $\Delta_1 = 0.008$, $\mu = 0.06$.

asynchronous quasi-periodicity.

6 Control of the chaos robustness via the dissipative coupling

As was mentioned above, a variation of Δ for the used form of the individual Rössler oscillator leads to the situation when both the chaotic regimes and windows of periodic regimes are possible, see Fig. 3. When there are several oscillators with different frequency parameters as in the system (3), a periodic regime occurs consistently in different oscillators with variation of Δ. Therefore, at a very small coupling in Fig. 12, there are windows of hyper-

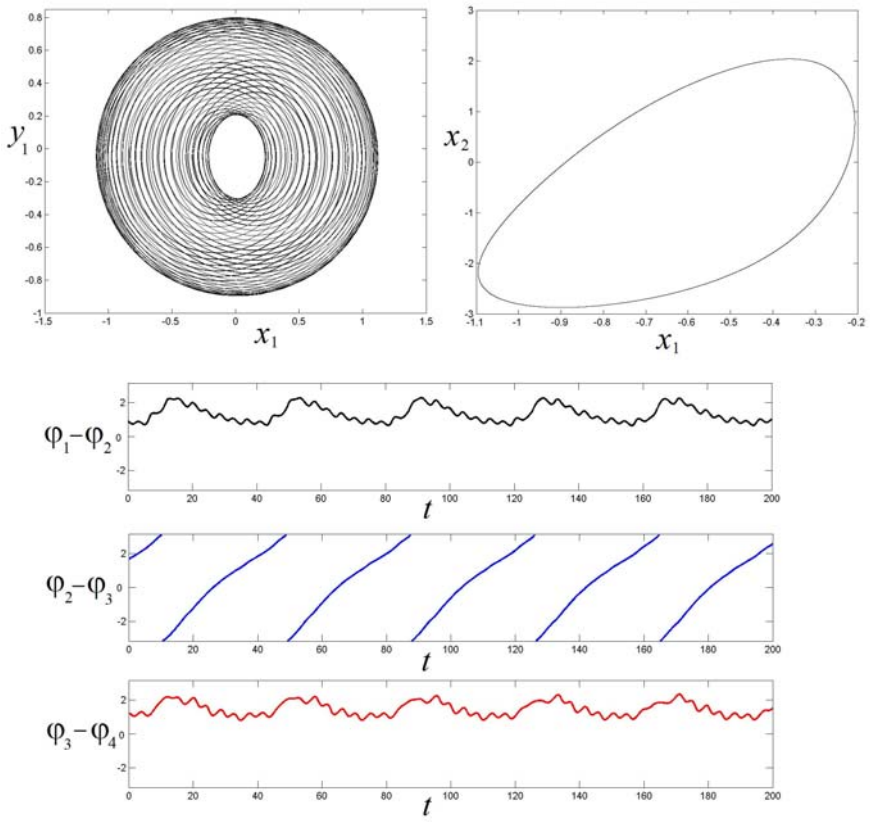

Figure 18: Phase portrait, Poincaré section and plots of three relative phases as functions of time at $\Delta_1 = 0.5$, $\mu = 0.145$.

chaos HC3 inside the domain of hyperchaos HC4. The reason is in the fact that one or another individual oscillator is inside the window of periodical regime with variation of Δ. Even hyperchaos HC2 is possible, which means that two individual oscillators are in the periodical regimes. This picture is actually quite typical and responds to the well-known nonrobust property of the chaotic systems [28]. The corresponding plots of Lyapunov exponents for the nonrobust systems are highly jagged.

However, these windows disappear quickly with an increase in the coupling, as Fig. 12 shows. Therefore, it is interesting to consider the plots of Lyapunov exponents as functions of the frequency parameter Δ at a very small (Fig. 19a) and not high, but also not so small coupling (Fig. 19b). Comparing Figs. 19a,b, we note that the plots of Lyapunov exponents be-

come less jagged. Thus, the dissipative coupling can be a factor that increases a degree of robustness for the observed chaos. This result is important for applications.

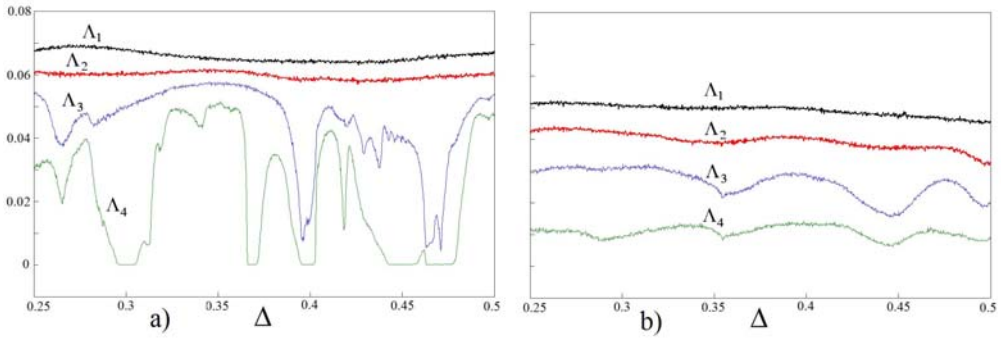

Figure 19: Plots of Lyapunov exponents illustrating an increase of the chaos robustness in the ensemble of oscillators; a) $\mu = 0.003$, b) $\mu = 0.025$.

7 Network of five Rössler chaotic oscillators

It is interesting to know if the observed regularities are saved with an increase in the number of oscillators. To answer this question, we consider a network of five Rössler chaotic oscillators. In this case, it is reasonable to take into account a non-identity of the parameter r, which is responsible for the excitation degree of the individual oscillators:

$$\begin{aligned} \dot{x}_n &= -(1 + \tfrac{n-1}{4}\Delta)y_n - z_n, \\ \dot{y}_n &= (1 + \tfrac{n-1}{4}\Delta)x_n + py_n + \tfrac{\mu}{4}\textstyle\sum_{i=1}^{5}(y_i - y_n), \\ \dot{z}_n &= q + (x_n - r_n)z_n. \end{aligned} \tag{4}$$

The chart of Lyapunov exponents for the system (4) is shown in Fig. 20. Its structure is close to that in case of four coupled oscillators and is complicated by an emergence of new regimes. In particular, there is a possibility of five-frequency tori T5. At high frequency mismatch (right edge of the chart in Fig. 20), there is a cascade of quasi-periodic Hopf bifurcations on the basis of tori of increasing dimension, which corresponds to the Landau–Hopf scenario [14,26-27]. But this scenario takes place in a narrow range of the coupling parameter, because new resonances occur rapidly enough.

However, we note the fact of possible Landau–Hopf scenario and cascade of quasi-periodic bifurcations of invariant tori in the system of coupled chaotic oscillators.

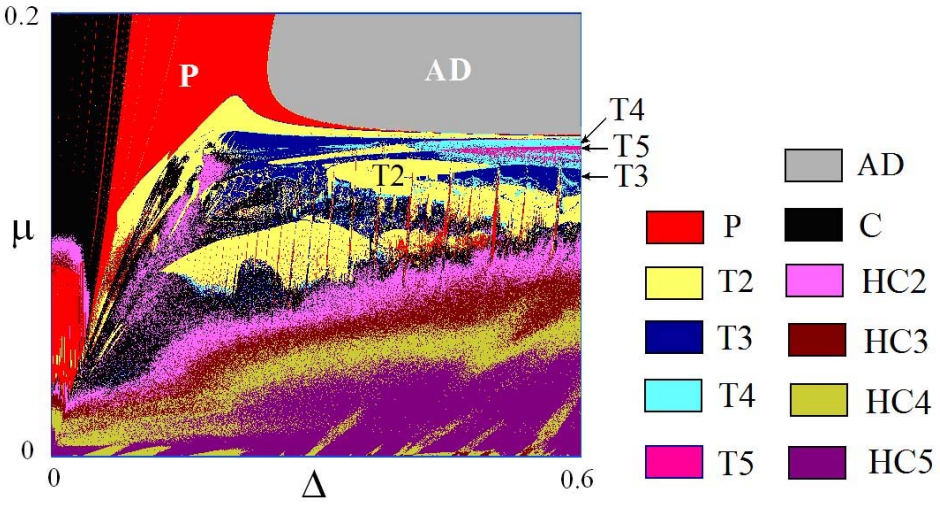

Figure 20: Chart of Lyapunov exponents for the network of five chaotic oscillators (4); $p = 0.15$, $q = 0.4$, $r_1 = 7.3$, $r_2 = 7.6$,$r_3 = 7.9$, $r_4 = 8.2$, $r_5 = 8.5$.

8 The frequency detuning parameters plane

So far, our research has focused on studying the "coupling - frequency detuning" parameters plane of the chaotic oscillators. It is interesting to consider the frequency detuning parameters space. To this end, let us return to the case of a chain of three coupled oscillators (2). Fig. 21 illustrates the change in the (Δ_1, Δ_2) parameter plane with increasing coupling.

You can see that at low coupling Fig. 21 presents only the chaotic regimes with different numbers of positive Lyapunov exponents. At the value μ=0.06 of the coupling parameter along with the chaotic there arise quasi-periodic regimes T2 and T3, Fig. 21b. The domains of two-frequency modes form numerous bands organized according to the principle of the resonance web. Note that two of the broadest bands T2 correspond to resonance conditions

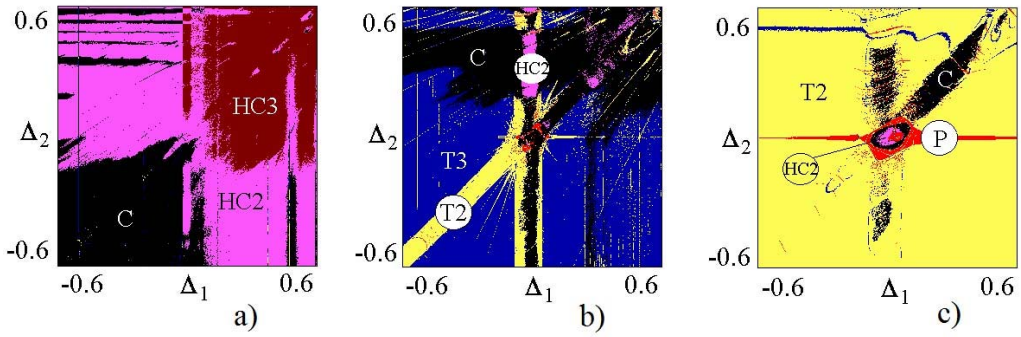

Figure 21: The plane of frequency detunings of three Rössler chaotic oscillators (2); $\mu = 0.02$ (a), $\mu = 0.06$ (b), $\mu = 0.1$ (c).

of equality for the frequencies of the first and second oscillators ($\Delta_1 = 0$), and the second and third ($\Delta_1 = \Delta_2$), respectively.

At still higher coupling in Fig. 21c the two-frequency quasi-periodicity modes T2 begin to dominate. In domains that correspond to the above resonances the chaotic regimes are observed now. In the neighborhood of the origin the complete synchronization region appears, which corresponds to the periodic regime P.

Note that the picture of the main resonance bands in Fig. 21b and the view of the external borders of the area of a complete synchronization on Fig. 21c are to some extent similar to the much simpler case of three coupled van der Pol oscillators, see Fig. 1 in [15].

9 Conclusion

In this paper, we show that the high-dimensional quasi-periodicity is characteristic not only for the ensembles of regular oscillators, but also for the chaotic oscillators with dissipative coupling. High-dimensional tori arise in the system of three, four and five coupled chaotic oscillators. Their Fourier spectra look like the classical spectra for the quasi-periodicity with the appropriate number of independent frequency components. An emergence of three-frequency regimes with a decrease in the coupling occurs usually as a result of a quasi-periodic Hopf bifurcation. With further decrease in the coupling, a set of resonance tori of different dimensions occurs through saddle-node

bifurcations. Inside the resonance domains, torus-doubling bifurcations with the subsequent fractalization and destruction are typical with a decrease in the coupling. However, an emerging resonance picture in the parameter plane is very complex and much more complicated than this one for the interacting regular oscillators. At high frequency mismatches of the subsystems, a cascade of subsequent quasi-periodic Hopf bifurcations for higher-dimensional tori may be observed in a certain range of the parameters.

What is the nature of high-dimensional quasi-periodicity in the coupled chaotic systems? We assume that it is caused by the possibility of a great number of unstable limit cycles embedded in the chaotic attractors. Interaction between the subsystems is the cause of their transformation into invariant tori, and high dissipative coupling stabilizes them. However, this hypothesis requires further consideration.

This work was supported by the Russian Foundation for Basic Research grant No.14-02-00085 and by RF President program for Leading Russian research schools NSh-1726.2014.

References

[1] Heinrich, G., Ludwig, M., Qian, J., Kubala, B. and Marquardt, F., Collective Dynamics in Optomechanical Arrays, *Phys. Rev. Lett.*, 2011, vol.107, 043603.

[2] Zhang, M., Wiederhecker, G.S., Manipatruni, S., Barnard, A., McEuen, P. and Lipson, M., Synchronization of Micromechanical Oscillators Using Light, *Phys. Rev. Lett.*, 2012, vol.109, 233906.

[3] Temirbayev, A., Nalibayev, Y.D., Zhanabaev, Z.Z., Ponomarenko, V.I. and Rosenblum, M., Autonomous and Forced Dynamics of Oscillator Ensembles with Global Nonlinear Coupling: An Experimental Study, *Phys. Rev. E*, vol.87, 2013, 062917.

[4] Martens, E.A., Thutupalli, S., Fourrière, A. and Hallatschek, O., Chimera States in Mechanical Oscillator Networks, *Proceedings of the National Academy of Sciences of the United States of America*, 2013, vol.110, pp.10563-10567.

[5] Tinsley, M.R., Nkomo, S. and Showalter, K., Chimera and Phase-Cluster States in Populations of Coupled Chemical Oscillators, *Nature Physics*, 2012, vol.8, pp.662-665.

[6] Vlasov, V. and Pikovsky, A., Synchronization of a Josephson junction array in terms of global variables, *Phys. Rev. E*, 2013, vol.88, 022908.

[7] Lee, T.E. and Cross, M.C., Pattern Formation with Trapped Ions, *Phys. Rev. Lett.*, 2011, vol.106, 143001.

[8] Lee, T.E. and Sadeghpour, H.R., Quantum Synchronization of Quantum van der Pol Oscillators with Trapped Ions, *Phys. Rev. Lett.*, 2013, vol.111, 234101.

[9] Grebogi, C., Ott, E. and Yorke, J.A., Attractors on an N-torus: Quasiperiodicity versus chaos, *Physica D*, 1985, vol.15, pp.354–373.

[10] Linsay, P.S. and Cumming, A.W., Three-frequency quasiperiodicity, phase locking, and the onset of chaos, *Physica D*, 1989, vol.40, pp.196-217.

[11] Battelino, P.M., Grebogi, C., Ott, E. and Yorke, J.A., Chaotic attractors on a 3-torus, and torus break-up, *Physica D*, 1989, vol.39, pp.299-314.

[12] Baesens, ., Guckenheimer, J., Kim, S. and MacKay, R.S., Three coupled oscillators: mode locking, global bifurcations and toroidal chaos, *Physica D*, 1991, vol. 49, pp.387-475.

[13] Emelianova, Yu.P., Kuznetsov, A.P., Sataev, I.R. and Turukina, L.V., Synchronization and multi-frequency oscillations in the low-dimensional chain of the self-oscillators, *Physica D*, 2013, vol.244, pp.36-49.

[14] Kuznetsov, A.P., Kuznetsov, S.P., Sataev, I.R. and Turukina, L.V., About Landau-Hopf scenario in a system of coupled self-oscillators, *Phys. Lett. A*, 2013, vol.377, pp.3291-3295.

[15] Emelianova, Yu.P., Kuznetsov, A.P., Turukina, L.V., Sataev, I.R. and Chernyshov, N.Yu., A structure of the oscillation frequencies parameter space for the system of dissipatively coupled oscillators, *Commun. Nonlinear Sci. Numer. Simul.*, 2014, vol.19, pp.1203-1212.

[16] Xiao-Wen, L., Zhi-Gang, Z., Phase Synchronization of Coupled Rossler Oscillators: Amplitude Effect, *Commun. Theor. Phys.*, 2007, vol.47, pp. 265–269.

[17] Pazó, D., Sánchez, E. and Matías, M. A., Transition to high-dimensional chaos through quasiperiodic motion, *Internat. J. Bifur. Chaos Appl. Sci. Engrg.*, 2001, vol. 11, pp.2683-2688.

[18] Pazó, D. and Matías, M.A., Direct transition to high-dimensional chaos through a global bifurcation, *Europhys. Lett.*, 2005, vol.72, pp. 176-182.

[19] Rosenblum, M.G., Pikovsky, A.S. and Kurths, J., Phase Synchronization of Chaotic Oscillators, *Phys. Rev. Lett.*, 1996, vol.76, pp.1804-1807.

[20] Osipov, G.V., Pikovsky, A.S., Rosenblum, M.G. and Kurths, J., Phase synchronization effects in a lattice of nonidentical Rössler oscillators, *Phys. Rev. E*, 1997, vol.55, pp.2353-2361.

[21] Pikovsky, A., Rosenblum, M. and Kurths, J., *Synchronization. A Universal Concept in Nonlinear Sciences*, Cambridge University Press, 2001.

[22] Vitolo, R., Broer, H. and Simó, C., Routes to chaos in the Hopf-saddle-node bifurcation for fixed points of 3D-diffeomorphisms, *Nonlinearity*, 2010, vol.23, pp.1919-1947.

[23] Broer, H., Simó, C. and Vitolo, R., Hopf-saddle-node bifurcation for fixed points of 3D-diffeomorphisms: Analysis of a resonance "bubble", *Physica D*, 2008, vol.237, pp. 1773-1799.

[24] Broer, H., Simó, C. and Vitolo, R., The Hopf-saddle-node bifurcation for fixed points of 3D-diffeomorphisms: the Arnol'd resonance web, *Bulletin of the Belgian Mathematical Society - Simon Stevin*, 2008, vol.15, 5, pp. 769-787.

[25] Vitolo, R., Broer, H. and Simó, C., Quasi-periodic bifurcations of invariant circles in low-dimensional dissipative dynamical systems, *Regular and Chaotic Dynamics*, 2011, vol. 16, 1-2, pp. 154-184.

[26] Landau, L.D., On the problem of turbulence, *Dokl. Akad. Nauk SSSR*, 1944, vol. 44, p.339-342.

[27] Hopf, E., A mathematical example displaying the features of turbulence, *Communications on Pure and Applied Mathematics*, 1948, vol.1, pp.303-322.

[28] Kuznetsov, S.P., *Hyperbolic Chaos: A Physicist's View*. Higher Education Press: Beijing and Springer: Heidelberg, Dordrecht, London, New York, 2011. 320p.